

## 2 **Conceptual Design of Reciprocating Probes and** 3 **Material-Testing Manipulator for Tokamak COMPASS** 4 **Upgrade**

---

5 **S. Lukes,<sup>a,1</sup> J. Horacek,<sup>b,2</sup> V. Veselovsky,<sup>b,2</sup> P. Vondracek,<sup>b,2</sup> D. Sestak,<sup>b,2</sup> J. Adamek,<sup>b,2</sup> V.**  
6 **Weinzettl,<sup>b,2</sup> I. Duran<sup>b,2</sup>**

7 <sup>a</sup>*FNSPE, Czech Technical University in Prague,*  
8 *Brehova 7, 115 19 Prague 1, Czech Republic.*

9 <sup>b</sup>*Institute of Plasma Physics of the CAS,*  
10 *Za Slovankou 1782/3, 182 00 Prague 8, Czech Republic*

11 *E-mail: [lukessam@fjfi.cvut.cz](mailto:lukessam@fjfi.cvut.cz)*

12 **ABSTRACT:** Three new in-vessel manipulators are designed and built for the new COMPASS Upgrade  
13 tokamak with uniquely high vessel temperature (250-500 °C) and heat flux density (perpendicular  
14 to divertor surface  $q_{\perp} \sim 80 \text{ MW/m}^2$  and  $q_{\parallel} \sim \text{GW/m}^2$  at separatrix), which challenges the edge  
15 plasma diagnostics. Here we show their detailed engineering designs supported by heat conduction  
16 and mechanical models.

17 Deep reciprocation of electrostatic probes near the separatrix should be possible by optimizing  
18 older concepts in a) the head and probe geometry, b) strongly increasing the deceleration up to  
19 100× gravity by springs and strengthening the manipulator mechanical structure. One reciprocates  
20 close to the region of edge plasma influx (the outer midplane), the other at the plasma sink (between  
21 the outer divertor strike point and X-point), for studying the plasma divertor (impurity-seeded)  
22 detachment and liquid metal vapor transport. Both probe heads are equipped with a set of ball-pen  
23 and Langmuir probes, measuring reliably extremely fast ( $10^{-6}$  s) and local (1 mm) plasma potential,  
24 density, electron temperature and heat flux and even ion temperature with  $10^{-5}$  s resolution.

25 The divertor manipulator (without reciprocation) will place various material test targets at the  
26 outer divertor. Unique will be its capability to increase 15× the surface heat flux with respect to the  
27 surrounding tungsten tiles just by controllable surface inclination of the test targets. We plan to test  
28 liquid metal targets where such inclined surface was found critical to achieve the desired mode with  
29 lithium vapor shielding. Even in the conservative expected performance of COMPASS Upgrade,  
30 we predict to reach and survive the EU DEMO relevant heat fluxes.

31 **KEYWORDS:** Plasma diagnostics - probes, Nuclear instruments and methods for hot plasma diag-  
32 nostics, Overall mechanics design

---

<sup>1</sup>FNSPE, Czech Technical University in Prague

<sup>2</sup>Institute of Plasma Physics of the CAS

---

## 33 Contents

34	<b>1 Introduction</b>	<b>1</b>
35	<b>2 Reciprocating Manipulators</b>	<b>2</b>
36	2.1 Design Review	2
37	2.2 Real-Time Depth Control	2
38	2.3 Accelerating the Reciprocation	4
39	2.4 Passive Radiation Cooling	4
40	<b>3 Material-Testing Manipulator</b>	<b>5</b>
41	<b>4 Conclusion</b>	<b>6</b>

---

## 42 1 Introduction

43 COMPASS Upgrade (COMPASS-U) will be a mid-size tokamak capable of generating fusion rel-  
44 evant plasma and containing it by high magnetic field (up to 5 T) configuration surrounded by  
45 uniquely high vessel temperatures 250-500 °C. Consequently, high density ( $\sim 10^{20} \text{ m}^{-3}$ ) thermonu-  
46 clear plasma will cause extreme heat stress on divertor surface reaching  $q_{\perp} \sim 80 \text{ MW/m}^2$  [8] and  
47 enormous heat flux density  $q_{\parallel} \sim \text{GW/m}^2$  at last closed flux surface (LCFS) in a discharge 2 s long.  
48 Such parameters of plasma equilibrium can be reached with the help of copper coils cooled in  
49 cryostat to the temperature of liquid nitrogen and 8 MW of plasma heating.

50 As the new opportunities for research evolves also the need for proper diagnostic and semi-  
51 automatic manipulator system is important. This lead to the re-design of an unfinished set of  
52 two independent fast reciprocating manipulators (signed as HRCP and XRCP) and to the design  
53 of one completely new slow & precise divertor tile manipulator (DivMat) capable of transporting  
54 heat-resistant materials (in between discharge) onto the divertor outer strike point.

55 Both pneumatic reciprocating manipulators will be equipped with a set of ball-pen (BPP) and  
56 Lanqmuir probes (LP). Combined set of BPPs and LPs is able to measure extremely fast (1 MHz [4])  
57 & locally plasma potential, plasma density, electron temperature without sweeping and heat flux  
58 density [3]. Even fast measurement  $10^{-5}$  s of ion temperature can be obtained when sweeping the  
59 BPP [4]. LP as one of the primary tools to study boundary plasma physics in experimental fusion  
60 reactors are in a direct contact with the plasma, hence in order to provide safe measurement in deep  
61 Scrape-Off Layer (SOL), fast reciprocation in/out is necessary. In later stages of COMPASS-U,  
62 exponentially increasing heat flux of decay length of  $<1$  mm is expected in region close to LCFS  
63 [5]. Therefore, an inaccuracy in the relative position of the probe to the plasma of the order of  
64 the decay length (1 mm) yields  $\approx 3\times$  higher heat flux on the probe. Such harsh conditions could  
65 quickly lead to melting of the probe or (even before the melting) to thermionic electron emission,  
66 which makes the measurement uncertain.

67 The paper is focused both on the engineering design of each manipulator and on the research  
 68 & ideas, which were made in order to reciprocate as deep as possible and to have as much universal  
 69 tile manipulator as possible.

## 70 2 Reciprocating Manipulators

71 Both HRCP and XRCP consist of similar mechanisms that allow mounted probes to protrude every  
 72  $\sim 10^{-1}$  s into plasma and if needed (figure 1a), retract outside of the tokamak, seal the vacuum,  
 73 review probe heads (figure 1b) or shift the whole manipulator along its short rails and remove probe  
 74 heads (figure 1c).

75 HRCP will scan low-field side midplane region, see figure 1d. How close to LCFS will depend  
 76 on implementation of secondary mechanisms (described below) allowing probes to measure SOL  
 77 turbulence transport and physics in high density plasma. XRCP will measure plasma properties in  
 78 divertor region, between X-point and outer strike-point, or can poloidally extend HRCP resolution  
 79 in scenarios with vertically inverted plasma. Its further usability lies in support of experiments  
 80 with prototype tiles on DivMat, especially on liquid metal experiments, where it is almost directly  
 81 (toroidally moved, see figure 1e) in contact with evaporated impurities from the tested tiles.

### 82 2.1 Design Review

83 The long ( $\approx 2.5$  m) slow movement is conducted by servomotors rotating long screw pole that causes  
 84 the movement of reciprocating system with probes and expansion/detraction of long vacuum bellow.  
 85 Probe heads are pushed by a long heat-resistant stainless steel rod, filled with Mineral Insulated  
 86 Cables sustaining high temperatures of vacuum chamber, in secondary support tube with the help  
 87 of three sliding plates. After reaching the parking position  $\approx 15$  cm outside LCFS, manipulators  
 88 wait for a discharge to reciprocate. Filling up  $2 \times 2$  pistons for each manipulator with helium gas,  
 89 probes reach velocity of 2.5 m/s and retract with deceleration of  $\approx 100$  m/s<sup>2</sup> (for a 3 kg probe head).  
 90 Piston filling can be adjusted, for example, to obtain more data at one significant position, where  
 91 conditions are not so demanding. Commonly to all pneumatic systems, this maximum speed is  
 92 limited by the friction of both the moving components and the helium gas.

At the same time, the probes must withstand double-exponential heat flux density profile of  
 decay lengths  $\lambda_q^{\text{near}}$ ,  $\lambda_q^{\text{far}}$  in radial direction  $r$  outside LCFS [5]

$$q_{\parallel}(r) = q_{\parallel}^{\text{LCFS}} \frac{R_q \exp(-r/\lambda_q^{\text{near}}) + \exp(-r/\lambda_q^{\text{far}})}{1 + R_q} \text{ reaches at LCFS } \sim \text{GW/m}^2, \quad (2.1)$$

93 where  $R_q$  is the ratio of *near* and *far* exponential decays of parallel heat flux at LCFS. In order  
 94 to measure more deep in the plasma, improvements are described below and can be additionally  
 95 implemented to the design.

### 96 2.2 Real-Time Depth Control

97 The decision was made that for safe and deep protrusion into plasma it is essential to check heat  
 98 deposited on the probe in real time. The first reciprocation of each plasma discharge will be safe and  
 99 shallow. Total heat  $Q$  deposited on the probe during its movement can be retrieved directly from the

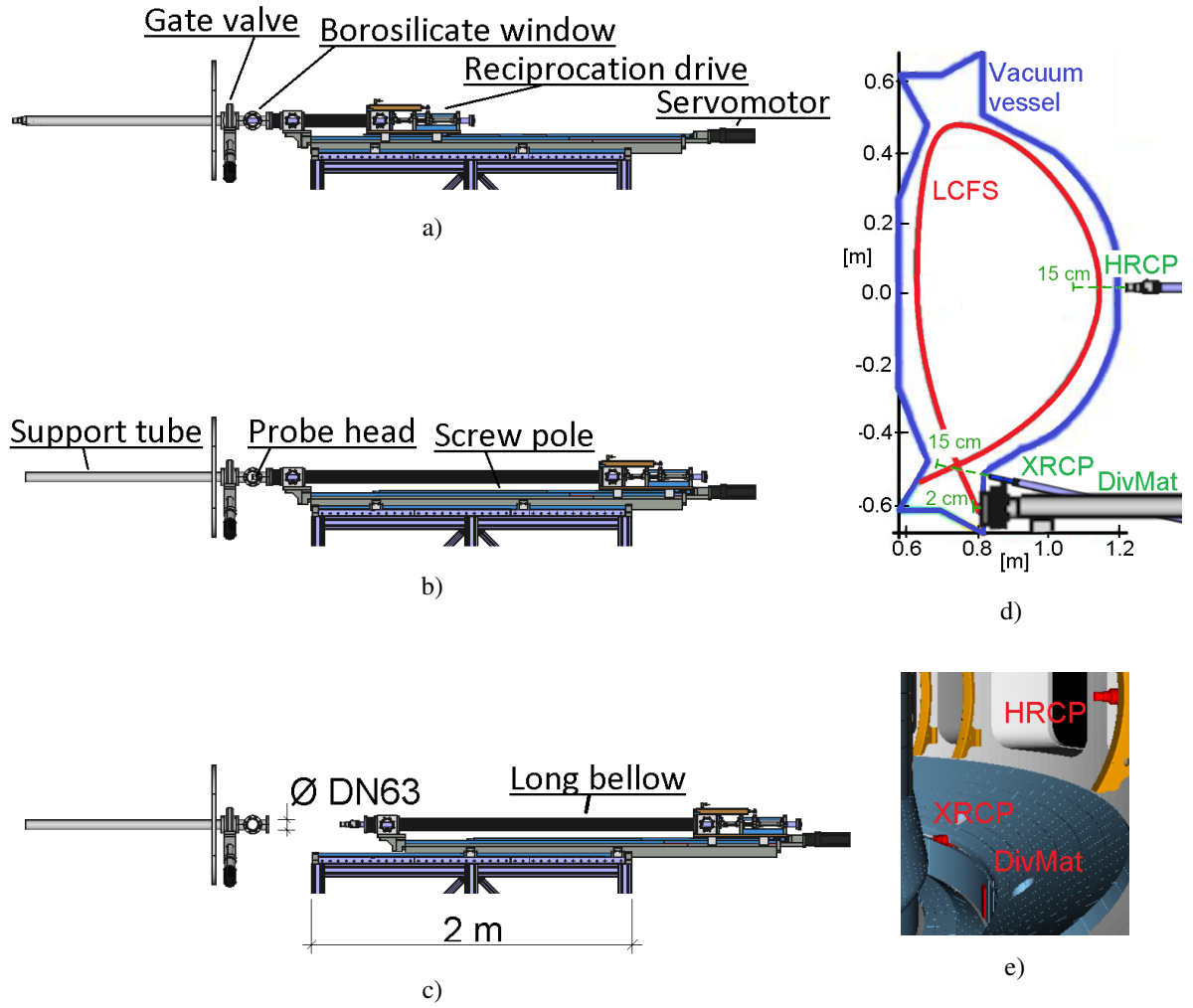


**Figure 1:** Schematic view on HRCP manipulator (XRCP and DivMat works on the same principle) in its three stages of operation. a) The probe waits in the parking position for a discharge followed by several reciprocations. b) Probe in the diagnostic window (possible check also between individual discharges). c) Manipulator ready to disassemble the probe. d) Poloidal cut showing the protrusion of all manipulators. e) Visible light camera view into the chamber.

100 ion saturation current  $I_{\text{sat}} = I_{-300\text{V}} / (1 - \exp([-300 - V_{\text{fl}}]/T_e))$  (from corrected current measured  
 101 at probe biased to -300 V, such correction is important during numerous instability events, such  
 102 as periodic Edge Localized Modes (ELMs), when  $\phi - 3T_e$  drops below  $\approx -200$  V) and electron  
 103 temperature  $T_e = (\phi_{\text{BPP}} - V_{\text{fl}})/2.2$  [3] as

$$Q = \int_{\text{reciprocation}} \gamma \cdot \frac{I_{\text{sat}}(t)}{A} \cdot T_e(t) dt, \quad (2.2)$$

104 where  $A$  is the effective area of the probe and  $\gamma$  is the sheath heat flux transmission coefficient.

Since the profile of incoming heat flux can be approximated as exponential (with decay length  $\lambda_q$  obtained from scaling laws [6, 7] and later calibrated for each mode), let us shift each plunge

depth by a distance  $\Delta r$  as

$$\Delta r = \lambda_q \log \left( \frac{P_{\text{prev}}}{P_{\text{next}}} \cdot \frac{Q_{\text{opt}}}{Q} \right) + \Delta d_{\text{LCFS}}, \quad (2.3)$$

105 where  $P_{\text{prev}}$ ,  $P_{\text{next}}$  is the external plasma heating power during *previous* and *next* plunge.  $\Delta d_{\text{LCFS}}$   
 106 is the shift of LCFS position compared to previous plunge and obtained from real-time magnetic  
 107 reconstruction EFIT. Even though EFIT has a large systematic error ( $\approx 1$  cm), relative shift  $\Delta d_{\text{LCFS}}$   
 108 can be calculated with sub-millimeter accuracy.  $Q_{\text{opt}}$  means an "optimum received heat" and will  
 109 be determined by trial and error practise in different operation regimes (L-mode, H-mode, ELMy  
 110 H-mode, ...), so that the surface probe temperature will be kept under its melting point throughout  
 111 the whole discharge. Servomotor of the slow movement (5-7 mm/s) is sufficiently fast to rearrange  
 112 the starting position of the fast reciprocation by  $\Delta r$  ( $\sim 0.5 - 1$  mm) during every of 10 to 20 plunges  
 113 for a 2 s long discharge.

### 114 2.3 Accelerating the Reciprocation

115 Since total amount of deposited heat increases with time spent in plasma, it is desirable to reciprocate  
 116 as fast as possible. This can be achieved by increasing both the deceleration in plasma and the  
 117 maximum velocity of the movement (which is reached within several centimeters for common  
 118 pneumatic systems). 1D heat equation simulation has been created in order to demonstrate the  
 119 situation.

120 We noticed the same behavior as seen on the Linear Servomotor Probe Drive System on  
 121 Alcator C-Mod tokamak [9]. The extremely variable heat flux density profile eq. (2.1) causes the  
 122 heat supplied to the probe after reaching the maximum velocity to be negligible compared to the  
 123 heat it receives during its turn around phase. Knowing that, we were able to propose improvements  
 124 to the existing design of the "slow" deceleration profile caused purely by increasing He gas pressure  
 125 in pistons. As shown in figure 2c, by adding a set of pre-loaded mechanical springs to the end  
 126 of the reciprocation mechanism, we acquired merely constant profile of deceleration (up to 100 g,  
 127 the stress limit for 3 kg of moving mass for our manipulator) causing probe to safely regain its  
 128 maximum velocity few times faster than in original setup. By doing so, we are able to keep surface  
 129 temperature  $T_{\text{max}}$  of graphite head under 1200 °C even when protruded 1 mm outside of LCFS, see  
 130 figure 2b where the heat flux perpendicular to the surface reaches 400 MW/m<sup>2</sup>.

### 131 2.4 Passive Radiation Cooling

132 Typically, reciprocations are so fast and discharge is so short (compared to time needed for energy  
 133 recovery in between discharges) that probes can take advantage of inertial cooling, i.e., only a thin  
 134 surface layer is heated and total gained heat during whole discharge is negligible to the total probe  
 135 heat capacity ( $< 20$  reciprocations on COMPASS-U causes temperature rise of  $\sim 1$  °C if distributed  
 136 along the whole probe mass), so the sudden temperature rise can be quickly ( $\sim \alpha_C l_{\text{head\&probe}}^2 = 10^2$  s,  
 137 where  $\alpha_C$  stands for thermal diffusivity of carbon composite) cooled down by its surroundings. But  
 138 on COMPASS-U (and future fusion reactors) vacuum vessel will be heated even up to 500 °C,  
 139 which limits self-cooling of the probe head to this temperature. Therefore, a system of passive  
 140 radiation cooling is further developed, cooling the pre-discharge head temperature down by 340 °C  
 141 (the entire temperature profile at figure 2b drops down by 340 °C).

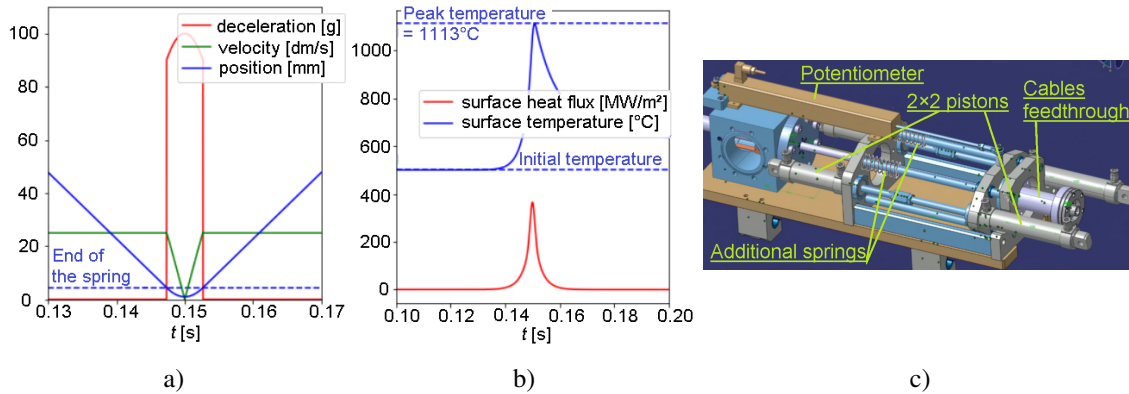


**Figure 2:** a), b) Simulated time evolution of one reciprocation for  $a_{\max} = 100$  g (981 m/s<sup>2</sup>),  $v_{\max} = 2.5$  m/s protruding 1 mm outside of LCFS in SOL with parameters  $\lambda_q^{\text{near, far}} = \{0.7; 7.0\}$  mm [6, 7] and  $R_q = 4$  [5]. c) The fast reciprocation pneumatic system of 2x2 pistons and two springs of total strength 90 N/mm.

142 Assuming a simple model of cylindrical graphite probe head coated by tungsten, heated  
 143 differently from both sides and cooled down by its thermal radiation into surrounding cooler.  
 144 Vacuum vessel at  $T_{\text{vessel}} = 500$  °C shines only to the front face of the head, resulting in heat influx  
 145  $P_{\text{front}} = 5$  W. Stainless steel outer support tube isolated by Multi-Layer Insulation causes the heating  
 146 of the head from behind  $P_{\text{behind}} = 4$  W. Due to only 1 W difference between  $P_{\text{front}}$  and  $P_{\text{behind}}$ ,  
 147 correction to the temperature gradient in the head is negligible thanks to its high heat conductivity.  
 148 Total heat influx  $P_{\text{front}} + P_{\text{behind}}$  can be radiated from the head, hence cooling it down to temperature  
 149 of 160 °C, by the help of surrounding radiation absorber at temperature of 20 °C. Radiation absorber  
 150 could be a metal tube (emissivity  $\varepsilon = 0.2$  is sufficient) wound around the head in its parking position  
 151 (behind the first wall of COMPASS-U) and cooled down by the outer cooling system connected via  
 152 additional tubing through the same vacuum vessel port as the manipulator uses.

### 153 3 Material-Testing Manipulator

154 Unlike two previous manipulators, DivMat is made from scratch, but it keeps the same simple design  
 155 of slow & long rotational screw pole with servomotor attached to a set of manually manipulated  
 156 rails. The reciprocating mechanism has been replaced by an additional rod (with square cross  
 157 section in order to stop its own rotation) that connects the tile holder with manual rotational  
 158 magnetic mechanism at the beginning of vacuum bellow, see figure 3a. This rod causes the tile to  
 159 be additionally positioned up to 2 cm with 1 mm precision with respect to the alignment of the tiles  
 160 in divertor region.

161 Tile attached to the holder at the end of manipulator slowly reaches the leading platform just  
 162 behind the vessel, which guides it to four corner joints serving as the main anchor fixing the tile  
 163 in one exact position. A copper plate leads from the tile holder to the manipulator, see figure 3b.  
 164 Electric current, induced during discharge by numerous instability events, is conducted by this plate  
 165 to the manipulator grounding. Such conductor minimizes  $j \times B$  force, which could mean serious  
 166 damage to the manipulator and surroundings.

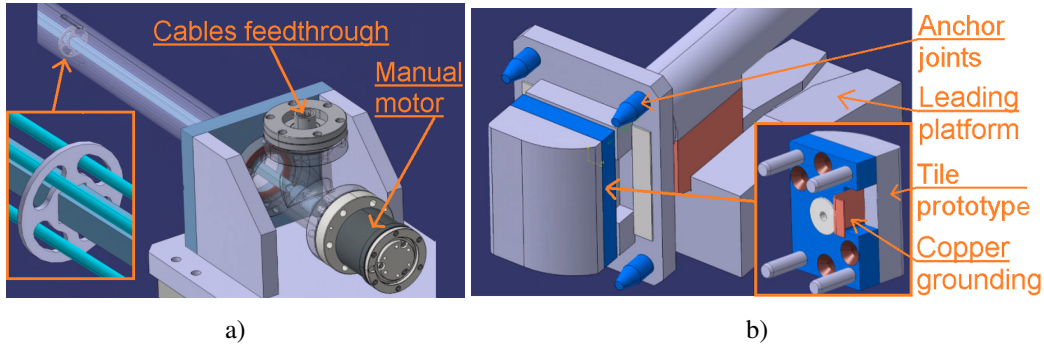


**Figure 3:** a) The beginning of the precise movement rod with moment magnetic feedthrough. b) Detail of the tile holder in parking position, showing the specially shaped tile for experiments (not only) on liquid metals.

167 Precise and rigid anchor of the tile is necessary since at later operational phases of COMPASS-  
 168 U with complete tungsten divertor heat flux at divertor tiles could reach even  $q_{\perp} = 80 \text{ MW/m}^2$   
 169 in stable H-mode [8]. Such high heat load is limiting even for estimated  $\sim 10^2 - 10^3$  ms long  
 170 discharges for most of materials. On the other hand, it provides a worldwide opportunity to further  
 171 investigate priority tasks for ITER with tungsten melting [10] and pre-damaged material testing [11],  
 172 or plasma deposition into gaps in between plasma facing components [1] (carried out in inner-wall  
 173 limited discharges on COMPASS with two follow-up experiments performed in divertor of AUG  
 174 and WEST). Experiment on liquid metals on COMPASS tokamak in 2019 [2, 7] was relevant thanks  
 175 to the simple shape of a quarter of a cylinder of the tile used there, see figure 3b. This particular  
 176 shape allowed to vary angle of impact with protrusion to plasma, which can also be ensured on  
 177 DivMat by the manually operated rod of precise movement. By doing so, DEMO relevant fluxes  
 178 ( $q_{\perp} = 160 \text{ MW/m}^2$  [8]) are achievable on the inclined tile surface even with long lasting ( $> 2$  s)  
 179 low power H-mode COMPASS-U conditions at  $q_{\perp} = 10 \text{ MW/m}^2$  on the surrounding divertor tiles.

## 180 4 Conclusion

181 Set of three independent manipulators is designed for the upcoming new COMPASS-Upgrade  
 182 tokamak. It consists of two fast reciprocating manipulators, horizontal HRCP scanning the midplane  
 183 region and XRCP scanning the region responsible for plasma detachment. Both of them can be  
 184 equipped with a set of additional springs allowing them to safely protrude 1 mm outside of LCFS  
 185 in a dense ( $\sim 10^{20} \text{ m}^{-3}$ ) thermonuclear deuterium plasma. If additional pre-cooling system is  
 186 accepted or in low power long lasting ( $> 2$  s) scenarios in L-mode, manipulators are capable of  
 187 protruding even inside LCFS. The third material testing manipulator (DivMat) is without the ability  
 188 to reciprocate but can fix the prototype tile (designed by DEMO engineers) in exact position ranging  
 189 up to 2 cm deeper than surrounding divertor tiles.

## 190 Acknowledgments

191 The authors would like to acknowledge projects COMPASS-U: Tokamak for cutting-edge fusion  
 192 research (No. CZ.02.1.01/0.0/0.0/16\_019/0000768), Czech Science Foundation 22-03950S and



193 student grant competition (SGS) for CTU in Prague: Study of plasma confinement by magnetic  
194 field in tokamak (SGS19/180/OHK4/3T/14).

## 195 References

- 196 [1] R. Dejarnac, et al., *Heat loads on poloidal and toroidal edges of castellated plasma-facing*  
197 *components in COMPASS*, Nucl. Fusion 58 066003 (2018),  
198 <https://doi.org/10.1088/1741-4326/aab973>.
- 199 [2] R. Dejarnac, et al., *Overview of power exhaust experiments in the COMPASS divertor with liquid*  
200 *metals*, Nuclear Materials and Energy 25 100801 (2020),  
201 <https://doi.org/10.1016/j.nme.2020.100801>.
- 202 [3] J. Adamek, et al., *Fast measurements of the electron temperature and parallel heat flux in ELMy*  
203 *H-mode on the COMPASS tokamak*, Nuclear Fusion, 57, no. 2 (2017)  
204 <http://dx.doi.org/10.1088/0029-5515/57/2/022010>.
- 205 [4] J. Adamek, et al., *Ion temperature measurements in the tokamak scrape-off layer with high temporal*  
206 *resolution*, Nucl. Fusion 61 036023 (2021).
- 207 [5] M. Kocan, et al., *Impact of a narrow limiter SOL heat flux channel on the ITER first wall panel*  
208 *shaping*, Nucl. Fusion 55 033019 (2015).
- 209 [6] T. Eich, et al., *Scaling of the tokamak near the scrape-off layer H-mode power width and implications*  
210 *for ITER*, Nucl. Fusion 53 093031 (2013).
- 211 [7] J. Horacek, et al., *Scaling of L-mode heat flux for ITER and COMPASS-U divertors, based on five*  
212 *tokamaks*, Nucl. Fusion 60 066016 (2020), <https://doi.org/10.1088/1741-4326/ab7e47>.
- 213 [8] J. Horacek, et al., *Predictive modelling of liquid metal divertor: from COMPASS tokamak towards*  
214 *Upgrade*, Phys. Scr. 96 124013 (2021), <https://doi.org/10.1088/1402-4896/ac1dc9>.
- 215 [9] D. Brunner, et al., *Linear servomotor probe drive system with real-time self-adaptive position control*  
216 *for the Alcator C-Mod tokamak*, Rev. Sci. Instrum. 88, 073501 (2017),  
217 <https://doi.org/10.1063/1.4990043>
- 218 [10] K. Krieger, et al., *Investigation of transient melting of tungsten by ELMs in ASDEX Upgrade*, Phys.  
219 *Scr.* 2017 014030 (2017), <https://doi.org/10.1088/1402-4896/aa8be8>.
- 220 [11] K. Krieger, et al., *Impact of H-mode plasma operation on pre-damaged tungsten divertor tiles in*  
221 *ASDEX Upgrade*, Phys. Scr. 2020 014037 (2020).